Inorganic Chemistry
Article

Inorg. Chem. **2009**, *48*, 5891–5900 **5891**
DOI: 10.1021/ic900198h

Nanometer Length-Dependent Triplet−Triplet Energy Transfers in Zinc(II) Porphyrin/*trans*-Bis(ethynylbenzene)Platinum(II) Oligomers

Li Liu,[†] Daniel Fortin, and Pierre D. Harvey*

Département de Chimie, Université de Sherbrooke, PQ, Canada J1K 2R1. [†]On leave from the Ministry of Education Key Laboratory for the Synthesis and Application of Organic Functional Molecules, School of Chemistry and Chemical Engineering, Hubei University, Wuhan 430062, People's Republic of China

Received January 31, 2009

The synthesis and characterization of organometallic oligomers of the type $[(p\text{-}C_6H_4)C{\equiv}CPt(P(n\text{-}Bu)_3)_2C{\equiv}C(p\text{-}C_6H_4)\text{-}$**Zn(P)**$]_n$ with the corresponding models $[(C_6H_5C{\equiv}C)Pt(P(n\text{-}Bu)_3)_2C{\equiv}C(p\text{-}C_6H_4)$**Zn(P)**$(p\text{-}C_6H_4)C{\equiv}CPt(P(n\text{-}Bu)_3)_2(C{\equiv}CC_6H_5)]$, where **Zn(P)** is zinc(II)-10,20-di(mesityl)- (n = 4, 9) or zinc(II)-10,20-di-*n*-pentyl-porphyrin (n = 3, 6, 9), are reported. The electronic spectra (absorption, excitation, emission, and transient absorption) and the photophysical properties (emission lifetimes and quantum yields) of these species in 2-methyltetrahyrofuran at 298 and 77 K are presented. Rates for triplet (T_1) energy transfer, k_{ET}, from the $[(p\text{-}C_6H_4C{\equiv}C)Pt(P(n\text{-}Bu)_3)_2(C{\equiv}C\text{-}p\text{-}C_6H_4)]$ spacer to **Zn(P)** vary from 2.4×10^4 to 1.3×10^6 s^{-1}. For the *n*-pentyl case, a rate dependence of oligomer size is noted as k_{ET} increases with the number of units, *n*. This phenomenon is interpreted by the presence of an excitonic process (i.e., delocalization of the energy along the **Zn(P)** array).

Introduction

The search for new metal-organic molecular and polymeric functional materials with optoelectronic applications continues to attract much attention.[1−8] Among these, conjugated metalated derivatives show a wide domain of intriguing properties useful for the development of optoelectronic devices such as organic light-emitting diodes,[2] photovoltaic cells,[3] sensors,[4] field-effect transistors,[5] and nonlinear optical devices.[6] Interests in understanding the photophysical properties of porphyrins and its electronic "communication" processes in the excited states such as energy and electron transfers inspired researchers to explore in more detail their behavior with respect to the photosynthesis mechanism.[9,10] An initial survey clearly showed that energy transfer

*To whom correspondence should be addressed. Tel.: 001-819-821-7092. Fax: 001-819-821-8017. E-mail: Pierre.harvey@usherbrooke.ca.

(1) (a) *Conjugated Polymeric Materials: Opportunities in Electronics, Optoelectronics and Molecular Electronics*; Brédas, J. L., Chance, R. R., Eds.; Kluwer Academic Publishers: Dordrecht, The Netherlands, 1990. (b) Coe, B. J.; Curati, N. R. M. *Comment Inorg. Chem.* **2004**, *25*, 147. (c) Chen, C. H.; Shi, J. *Coord. Chem. Rev.* **1998**, *171*, 161. (d) Low, P. J. *Dalton Trans.* **2005**, 2821. (e) Yam, V. W.-W. *Acc. Chem. Res.* **2002**, *35*, 555. (f) Wong, W.-Y. *Coord. Chem. Rev.* **2005**, *249*, 971. (g) Bunz, U. H. F.; Rubin, Y.; Tobe, Y. *Chem. Soc. Rev.* **1999**, *28*, 107. (h) Kingsborough, R. P.; Swager, T. M. *Prog. Inorg. Chem.* **1999**, *48*, 123. (i) Stott, T. L.; Wolf, M. O. *Coord. Chem. Rev.* **2003**, *246*, 89. (j) Abd-El-Aziz, A. S. *Macromol. Rapid Commun.* **2002**, *23*, 995.

(2) (a) Friend, R. H.; Gymer, R. W.; Holmes, A. B.; Burroughes, J. H.; Marks, R. N.; Taliani, C.; Bradley, D. D. C.; Dos Santos, D. A.; Brédas, J. L.; Lögdlund, M.; Salaneck, W. R. *Nature* **1999**, *397*, 121. (b) Baldo, M. A.; O'Brien, D. F.; You, Y.; Shoustikov, A.; Sibley, S.; Thompson, M. E.; Forrest, S. R. *Nature* **1998**, *395*, 151. (c) Baldo, M. A.; Thompson, M. E.; Forrest, S. R. *Pure Appl. Chem.* **1999**, *71*, 2095. (d) Lu, W.; Mi, B.-X.; Chan, M. C. W.; Hui, Z.; Che, C.-M.; Zhu, N.; Lee, S.-T. *J. Am. Chem. Soc.* **2004**, *126*, 4958. (e) Lin, Y.-Y.; Chan, S.-C.; Chan, M. C. W.; Hou, Y.-J.; Zhu, N.; Che, C.-M.; Liu, Y.; Wang, Y. *Chem. Eur. J.* **2003**, *9*, 1264. (f) Lupton, J. M.; Samuel, I. D. W.; Frampton, M. J.; Beavington, R.; Burn, P. L. *Adv. Funct. Mater.* **2001**, *11*, 287.

(3) (a) Halls, J. M.; Walsh, C. A.; Greenham, N. C.; Marseglia, E. A.; Friend, R. H.; Oratti, S. C.; Holmes, A. B. *Nature* **1995**, *376*, 498. (b) Yu, G.; Gao, J.; Hummelen, J. C.; Wudl, F.; Heeger, A. J. *Science* **1995**, *270*, 1789. (c) Chawdhury, N.; Younus, M.; Raithby, P. R.; Lewis, J.; Friend, R. H. *Opt. Mater.* **1998**, *9*, 498. (d) Younus, M.; Köhler, A.; Cron, S.; Chawdhury, N.; Al-Mandhary, M. R. A.; Khan, M. S.; Lewis, J.; Long, N. J.; Friend, R. H.; Raithby, P. R. *Angew. Chem., Int. Ed.* **1998**, *37*, 3036.

(4) (a) Yang, Q.-Z.; Wu, L.-Z.; Zhang, H.; Chen, B.; Wu, Z.-X.; Zhang, L.-P.; Tung, C.-H. *Inorg. Chem.* **2004**, *43*, 5195. (b) Kim, I.-B.; Erdogan, B.; Wilson, J. N.; Bunz, U. H. F. *Chem. Eur. J.* **2004**, *10*, 6247. (c) McQuade, D. T.; Pullen, A. E.; Swager, T. M. *Chem. Rev.* **2000**, *100*, 2537.

(5) (a) Sirringhaus, H.; Tessler, N.; Friend, R. H. *Science* **1998**, *280*, 1741. (b) Garnier, F.; Hajlaoui, R.; Yasser, A.; Svwastra, P. *Science* **1994**, *265*, 1684.

(6) (a) Long, N. J. *Angew. Chem., Int. Ed. Engl.* **1995**, *34*, 21. (b) Marder, S. R. In *Inorganic Materials*; Bruce, D. W., O'Hare, D., Eds.; Wiley: Chichester, U.K., 1996; p 121. (c) Barlow, S.; O'Hare, D. *Chem. Rev.* **1997**, *97*, 637. (d) Humphrey, M. G. *Coord. Chem. Rev.* **2004**, *248*, 725. (e) Nguyen, P.; Lesley, G.; Marder, T. B.; Ledoux, I.; Zyss, J. *Chem. Mater.* **1997**, *9*, 406. (f) Krivokapic, A.; Anderson, H. L.; Bourhill, G.; Ives, R.; Clark, S.; McEwan, K. J. *Adv. Mater.* **2001**, *13*, 652. (g) Zhou, G.-J.; Wong, W.-Y.; Cui, D.; Ye, C. *Chem. Mater.* **2005**, *17*, 5209.

(7) (a) Long, N. J.; Williams, C. K. *Angew. Chem., Int. Ed.* **2003**, *42*, 2586. (b) Nguyen, P.; Gomez-Elipe, P.; Manners, I. *Chem. Rev.* **1999**, *99*, 1515. (c) Manners, I. *Synthetic Metal-Containing Polymers*; Wiley-VCH: Weinheim, Germany, 2004. (d) Szafert, S.; Gladysz, J. A. *Chem. Rev.* **2003**, *103*, 4175. (e) Silverman, E. E.; Cardolaccia, T.; Zhao, X.; Kim, K. Y.; Haskins-Glusac, K.; Schanze, K. S. *Coord. Chem. Rev.* **2005**, *249*, 1491. (f) Wong, W.-Y. *J. Inorg. Organomet. Polym. Mater.* **2005**, *15*, 197. (g) Wong, W.-Y. *Comment Inorg. Chem.* **2005**, *26*, 39.

(8) (a) Wilson, S.; Dhoot, A. S.; Seeley, A. J. A. B.; Khan, M. S.; Köhler, A.; Friend, R. H. *Nature* **2001**, *413*, 828. (b) Chawdhury, N.; Köhler, A.; Friend, R. H.; Wong, W.-Y.; Lewis, J.; Younus, M.; Raithby, P. R.; Corcoran, T. C.; Al-Mandhary, M. R. A.; Khan, M. S. *J. Chem. Phys.* **1999**, *110*, 496.

(9) Jordan, P.; Fromme, P.; Witt, H. T.; Klukas, O.; Saenger, W.; Krauss, N. *Nature* **2001**, *411*, 909.

(10) Gust, D.; Moore, T. A.; Moore, A. L. *Acc. Chem. Res.* **2001**, *34*, 40.

Published on Web 06/11/2009

(ET) increases as the distance between the donor and acceptor porphyrins decreases.[11] Recently, heavy-metal-containing bis(ethynyl) linkers were used to form conjugated carbazole- and fluorene-based bis(ethynyl)−metal polymers (metal = platinum, gold, and mercury), and their emission spectroscopy and photophysics were investigated.[12] The key feature is that incorporation of a heavy metal in the backbone of the polymers can enhance intersystem crossing, hence leading to an increase in the population of the triplet states.

Bearing this in mind, we designed here several Pt acetylide conjugated systems combined with metalated porphyrins. A series of oligomers and polymers containing Pt acetylide and Zn porphyrins are synthesized and characterized, and their photophysical properties are investigated. To our knowledge, no other study of energy (donor−acceptor)-containing organometallic porphyrin polymers exist to date. We now wish to report the synthesis and characterization of nano-oligomers of the type $[(p\text{-}C_6H_4)C{\equiv}CPt(P(n\text{-}Bu)_3)_2C{\equiv}C(p\text{-}C_6H_4)\mathbf{Zn(P)}]_n$ with the corresponding models $[(C_6H_5C{\equiv}C)Pt(P(n\text{-}Bu)_3)_2C{\equiv}C(p\text{-}C_6H_4)\mathbf{Zn(P)}(p\text{-}C_6H_4)C{\equiv}C\text{-}Pt(P(n\text{-}Bu)_3)_2(C{\equiv}CC_6H_5)]$, where **Zn(P)** is zinc(II)-10, 20-di(2,4,6-trimethylphenyl)- or zinc(II)-10,20-*n*- dipentylporphyrin (Chart 1). The electronic spectra and the photophysical properties of these species in 2-methyltetrahydrofuran (2MeTHF) at 298 and 77 K are presented. A discussion on the triplet−triplet energy transfer, T_1 ET, from the $[(p\text{-}C_6H_4\text{-}C{\equiv}C)Pt\text{-}\ (P(n\text{-}Bu)_3)_2C{\equiv}C(p\text{-}C_6H_4)]$ chromophore to the porphyrin moiety is made. We find that the rate for T_1 ET for the olimer with largest number of repeating units is faster (1.35×10^6 s^{-1}). This work represents the first example of detailed investigations that address electronic communication in the backbone of a conjugated organometallic porphyrin-containing polymer.

Experimental Section

Materials. All reactions were carried out under a nitrogen atmosphere by using standard Schlenk techniques. Solvents were dried and distilled from appropriate drying agents under an inert atmosphere prior to use. Glassware was oven-dried at about 120 °C. All reagents and chemicals, unless otherwise stated, were purchased from commercial sources and used without further purification. The compounds 4-trimethylsilylethynylbenzaldehyde,[13] *meso*-substituted dipyrromethanes (5-mesityl- and 5-*n*-pentyldipyrromethane),[14] *trans*-chloro(ethynylbenzene)bis(tri*n*-butyl- phosphine)platinum (II),[15] and *trans*-$[Pt(P(n\text{-}Bu)_3)_2Cl_2]$[16] were prepared according to the literature methods.

5,15-Bis(mesityl)-10,20-bis(1,4-trimethylsilanylethynylbenzene)-zinc(II)porphyrin (T1). 5-Mesityldipyrromethane (2.98 g, 11.3 mmol) and 4-trimethylsilylethynylbenzaldehyde (2.28 g, 11.3 mmol) were dissolved in 125 mL of $CHCl_3$ under Ar in a one-neck round-bottom flask. $BF_3 \cdot O(Et)_2$ (54 μL) was added to initiate the condensation. The reaction mixture was stirred for 1 h under Ar. 2,3-Dichloro-5,6-dicyano-1,4-benzoquinone (DDQ; 2.56 g, 11.3 mmol) was added to the reaction mixture, and stirring was continued for another hour. The solvent was removed. A solution of $Zn(OAc)_2 \cdot 2H_2O$ (1.86 g, 8.47 mmol) in MeOH (18 mL) was added to the residue in $CHCl_3$ (100 mL), and the mixture was stirred and refluxed for 2 h. The crude reaction mixture was washed with H_2O and dried over $MgSO_4$. The crude product was then purified by using chromatography on silica gel with CH_2Cl_2/hexane (1:2) as a solvent. This afforded a red solid (1.85 g, 34.4%). ^{1}H NMR ($CDCl_3$, 400 MHz): δ 0.38 (s, 18 H), 1.82 (s, 12 H), 2.63 (s, 6H), 7.28 (s, 4H), 7.87 (d, 4H, J = 12 Hz), 8.17 (d, 4H, J = 12 Hz), 8.79 (d, 4H, J = 4.4 Hz), 8.84 (d, 4H, J = 4.4 Hz).

5,15-*n*-Pentyl-10,20-bis(1,4-trimethylsilanylethynylbenzene)-zinc(II)porphyin (T2). 5-*n*-Pentyldipyrromethane (2.14 g, 9.89 mmol) and 4-trimethylsilylethynyl- benzaldehyde (2.00 g, 9.89 mmol) were dissolved in 125 mL of $CHCl_3$ under Ar in a one-neck round-bottom flask. $BF_3 \cdot O(Et)_2$ (54 μL) was added to initiate the condensation. The reaction mixture was stirred for 1 h under Ar. DDQ (2.25 g, 9.89 mmol) was added to the reaction mixture, and stirring of the solution was continued for another hour. The solvent was removed. A solution of $Zn(OAc)_2 \cdot 2H_2O$ (1.63 g, 7.42 mmol) in MeOH (18 mL) was added to the residue in CH_2Cl_2 (100 mL), and the mixture was stirred and refluxed for 2 h. The crude reaction mixture was washed with H_2O and dried over $MgSO_4$. The crude product was purified by using chromatography on silica gel with CH_2Cl_2/hexane (1:2) as the solvent. This afforded a red solid (0.7066 g, 16.6%). ^{1}H NMR ($CDCl_3$, 400 MHz): δ 0.44 (s, 18 H), 0.88−1.00 (m, 6 H), 1.31−1.78 (m, 6H), 2.37−2.50 (m, 4H), 4.58−4.75 (m, 4H), 7.91 (d, 4H, J = 12 Hz), 8.07 (d, 4H, J = 12 Hz), 8.75 (d, 4H, J = 5.8 Hz), 9.27 (d, 4H, J = 6.0 Hz). ^{13}C NMR ($CDCl_3$, 100 MHz): δ 149.86, 148.64, 143.26, 134.32, 131.67, 130.12, 128.59, 122.10, 120.80, 118.85, 105.27, 101.69, 95.24, 38.68, 35.40, 32.87, 22.77, 14.18, 0.14. EI-MS m/z calcd for $C_{52}H_{56}N_4Si_2Zn$ $[M]^+$: 858.59. Found: 856.

5,15-Bis(1,4-ethynylbenzene)-10,20-bis(mesityl)zinc(II)porphyrin (L1). K_2CO_3 (1.34 g, 9.70 mmol) was added to a solution of **T1** (1.85 g, 1.94 mmol) in THF and MeOH (v/v = 1:1; 100 mL) and was stirred for 12 h. The solution was evaporated. The crude product was purified by column chromatography on silica gel with CH_2Cl_2/hexane (1:1) as the solvent to yield the pure ligand as a red solid (1.41 g, 90%). ^{1}H NMR ($CDCl_3$, 400 MHz): δ 1.83 (s, 12 H), 2.64 (s, 6 H), 3.31 (s, 2H), 7.29 (s, 4H), 7.88 (d, 4H, J = 12 Hz), 8.20 (d, 4H, J = 12 Hz), 8.80 (d, 4H, J = 4.4 Hz), 8.86 (d, 4H, J = 4.4 Hz). EI-MS m/z calcd for $C_{54}H_{40}N_4Zn$ $[M]^+$: 810.31. Found: 808.

5,15-Bis(1,4-ethynylbenzene)-10,20-di-*n*-pentylzinc(II)porphyrin (L2). K_2CO_3 (0.569 g, 4.12 mmol) was added to a solution of **T2** (0.707 g, 0.823 mmol) in a THF and MeOH (v/v = 1:1) solution (100 mL) and stirred for 12 h. The solution was evaporated. The crude product was purified by column chromatography on silica gel with CH_2Cl_2/hexane (1:1) as the solvent, to yield the pure ligand as a red solid (0.500 g, 85%). ^{1}H NMR ($CDCl_3$, 400 MHz): δ 0.97−0.99 (m, 6 H), 1.52−1.80 (m, 4 H), 2.42−2.58 (m, 4H), 3.28 (s, 2H), 4.82−4.93 (m, 4H), 7.88 (d, 4H, J = 6.0 Hz), 8.15 (d, 4H, J = 6.0 Hz), 8.91 (d, 4H, J = 4.4 Hz), 9.51 (d, 4H, J = 4.4 Hz). ^{13}C NMR ($CDCl_3$, 100 MHz): δ 150.18, 149.35, 148.81, 143.64, 134.26, 131.86, 131.55, 130.30, 128.89, 121.18, 83.80, 78.03, 38.70, 35.60, 32.84, 22.77, 14.16. EI-MS m/z calcd for $C_{54}H_{40}N_4Zn$ $[M]^+$: 714.23. Found: 712.

(11) Faure, S.; Stern, C.; Guilard, R.; Harvey, P. D. *J. Am. Chem. Soc.* **2004**, *126*, 1253.
(12) (a) Wong, W.-Y. *J. Inorg. Organomet. Polym. Mater.* **2005**, *15*, 197. (b) Wong, W.-Y.; Ho, C. L. *Coord. Chem. Rev.* **2006**, *250*, 2627. (c) Powell, C. E.; Humphrey, M. G. *Coord. Chem. Rev.* **2004**, *248*, 725. (d) Abd-El-Aziz, A. S. *Macromol. Rapid Commun.* **2002**, *23*, 995. (e) Long, N. J.; Williams, C. K. *Angew. Chem.* **2003**, *115*, 2690. *Angew. Chem., Int. Ed.* **2003**, *42*, 2586. (f) Manners, I. *Science* **2001**, *294*, 1664. (g) Bunz, U. H. F. *Chem. Rev.* **2000**, *100*, 1605. (h) Wong, W.-Y. *Dalton Trans.* **2007**, 4495. (i) Wong, W.-Y. *Macromol. Chem. Phys.* **2008**, *209*, 14.
(13) Austin, W. B.; Bilow, N.; Kelleghan, W. J.; Lau, K. S. Y. *J. Org. Chem.* **1981**, *46*, 2280.
(14) Laha, J. K.; Dhanalekshmi, S.; Taniguchi, M.; Ambroise, A.; Lindsey, J. S. *Org. Proc. Res. Dev.* **2003**, *7*, 799.
(15) Miki, S.; Ohno, T.; Iwasaki, H.; Yoshida, Z. *J. Phys. Org. Chem.* **1988**, *1*, 333.
(16) Kauffman, B.; Teter, L. A.; Huheey, J. E. *Inorg. Synth.* **1963**, *7*, 245.

Chart 1

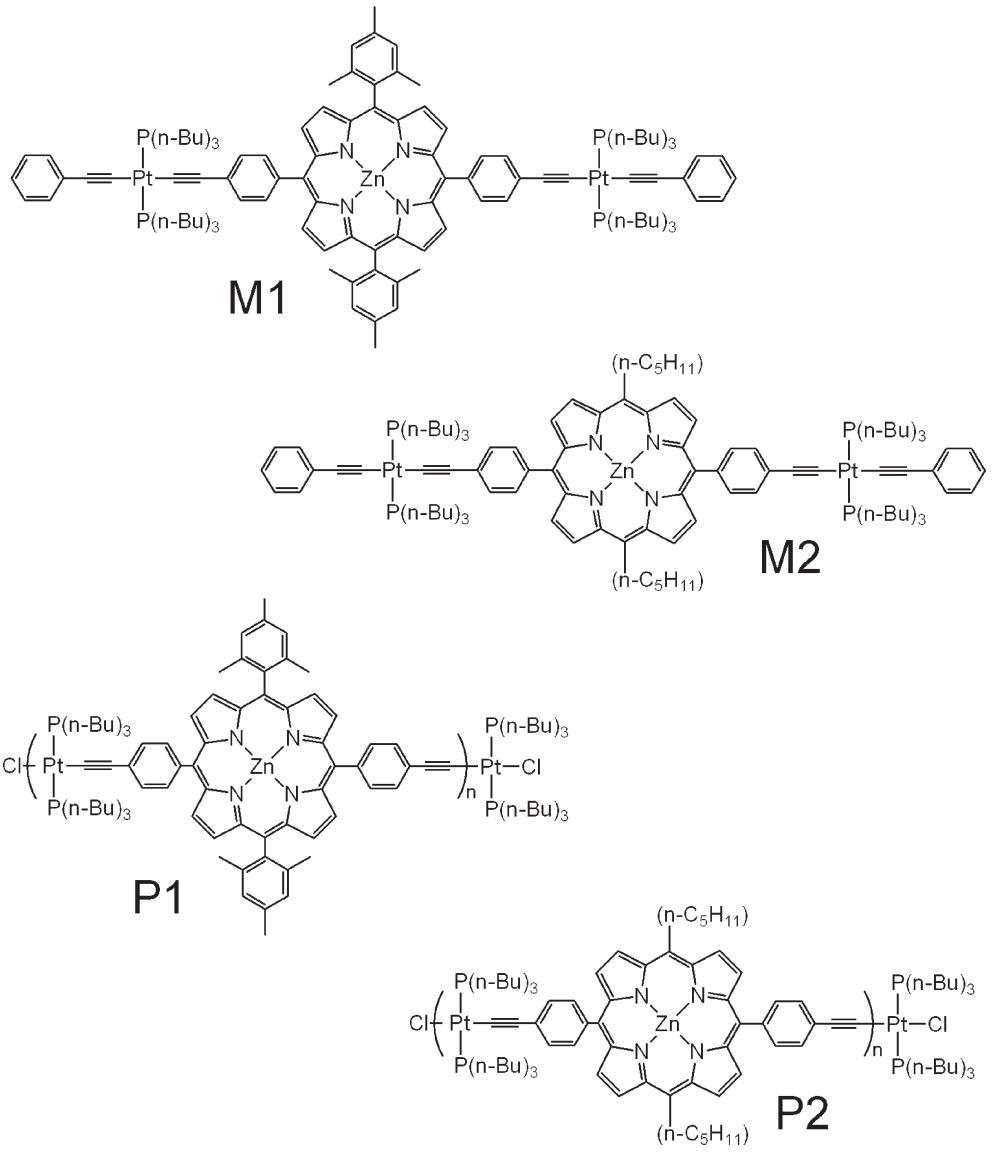

Poly[5,15-(*trans*-bis(1,4-ethynylbenzene)bis(tri-*n*-butylphosphine)-platinum(II))-10,20-bis(mesityl)zinc(II)porphyrin] (P1). A mixture of *trans*-Pt(P(*n*-Bu)$_3$)$_2$Cl$_2$ (200 mg, 0.298 mmol) and 1 equiv of **L1** (242 mg, 0.298 mmol) was dissolved in ^{i}Pr$_2$NH−CH$_2$Cl$_2$ (50 mL, 1:1, v/v), and CuI (3 mg) was subsequently added. After stirring for 24 h at 298 K, all of the volatiles were removed under reduced pressure. The residue was redissolved in CH$_2$Cl$_2$ and filtered through a short silica column using CH$_2$Cl$_2$ as a solvent to give a yellow solution of the polymeric material. The monomer was removed by adding MeOH to induce a precipitation of the polymer. The monomer remained soluble. The solid (i.e., the polymer) was filtered and washed with MeOH. The precipitation and washing were performed three times, to afford a red solid in 54.0% yield (227 mg). ^{1}H NMR (CDCl$_3$, 400 MHz): δ 1.05−1.09 (m, 18 H), 1.22−1.26 (m, 12 H), 1.54−1.60 (m, 12 H), 2.17 (s, 12 H), 2.37−2.39 (m, 12 H), 2.65 (s, 6H), 7.26−7.30 (m, 4H), 7.75 (d, 4H, J = 10.4 Hz), 8.14 (d, 4H, J = 10.4 Hz), 8.79 (d, 4H, J = 6.3 Hz), 8.95 (d, 4H, J = 6.3 Hz). ^{31}P NMR (CDCl$_3$, 160 MHz): δ 4.56 ($^1J_{Pt-P}$ = 3106 Hz). Elem anal. calcd (%) for $(C_{78}H_{92}N_4P_2PtZn)_n$: C, 66.54; H, 6.59; N, 3.98. Found: C, 63.49; H, 5.63; N, 3.14. GPC (THF): M_w = 24531, M_n = 13262.

Poly[5,15-(*trans*-bis(1,4-ethynylbenzene)bis(tri-*n*-butylphosphine)-platinum(II))-10,20-bis(*n*-pentyl)zinc(II)porphyrin] (P2). A mixture of *trans*-Pt(P(*n*-Bu)$_3$)$_2$Cl$_2$ (115 mg, 0.172 mmol) and 1 equiv of **L2** (123 mg, 0.172 mmol) was dissolved in ^{i}Pr$_2$NH−CH$_2$Cl$_2$ (50 mL, 1:1, v/v), and CuI (3 mg) was subsequently added. After stirring for 12 h at different temperatures (25, 80, and 110 °C producing three oligomers of different lengths), all of the volatiles were removed under reduced pressure. The residue was redissolved in CH$_2$Cl$_2$ and filtered through a short silica column using CH$_2$Cl$_2$ as a solvent to give a yellow solution of the polymeric material. The monomer was removed by adding MeOH to induce a precipitation of the polymer. The monomer remained soluble. The solid (i.e., the polymer) was filtered and washed with MeOH. The precipitation and washing were performed three times, to afford a red solid in 70.5% yield (158 mg). ^{1}H NMR (CDCl$_3$, 400 MHz): δ 0.98−1.07 (m, 36 H), 1.53−1.65 (m, 28 H), 1.73−1.86 (m, 28 H), 2.28−2.36 (m, 24 H), 2.55−2.57 (m, 4 H), 5.00−5.05 (br s, 4 H), 7.26−7.34 (m, 10 H), 7.76 (br s, 4H), 8.11 (br s, 4H), 9.09 (br s, 4H), 9.56 (br s, 4H). ^{13}C NMR (CDCl$_3$, 100 MHz): δ 150.12, 149.27, 139.84, 134.19, 132.09, 130.82, 128.89, 128.49, 127.86, 124.82, 120.48, 119.96, 109.47, 109.11, 108.90, 108.06, 38.76, 35.73, 32.87, 26.47, 24.52, 24.00, 22.84, 14.18, 13.95. ^{31}P NMR (CDCl$_3$, 160 MHz): δ 4.72 ($^1J_{Pt-P}$ = 3102 Hz). Elem anal. calcd (%) for $(C_{70}H_{93}N_4P_2PtZn)_n$: C,

64.04; H, 7.14; N, 4.27. Found: C, 63.84; H, 6.94; N, 3.98. GPC (THF): $M_w = 21460$, $M_n = 9908$.

5,15-Bis(*trans*-bis(1,4-ethynylbenzene)bis(tri-*n*-butylphosphine)-platinum(II))-10,20-bis(mesityl)zinc(II)porphyrin (M1). Treatment of **L1** (119 mg, 0.147 mmol) with 2 equiv of *trans*-phenylethynylchlorobis(tri-*n*-butylphosphine) platinum(II) (216.5 mg, 0.2940 mmol) for 12 h at 298 K, in the presence of CuI (3 mg), in $^iPr_2NH-CH_2Cl_2$ (50 mL, 1:1, v/v) gave the title complex as a red solid in 74.5% yield (250 mg) after purification on a silica column using *n*-hexane/CH_2Cl_2 (40:60, v/v) as a solvent. ^{1}H NMR ($CDCl_3$, 400 MHz): δ 1.01−1.05 (m, 36 H), 1.54−1.61 (m, 24 H), 1.74−1.75 (m, 24 H), 1.87 (s, 12 H), 2.29−2.30 (m, 24 H), 2.67 (s, 6 H), 7.24−7.36 (m, 12 H), 7.68 (d, 4H, $J = 10.4$ Hz), 8.11 (d, 4H, $J = 10.4$ Hz), 8.81 (d, 4H, $J = 6.3$ Hz), 8.99 (d, 4H, $J = 6.3$ Hz). ^{13}C NMR ($CDCl_3$, 100 MHz): δ 150.11, 149.79, 139.26, 137.40, 134.26, 132.38, 130.82, 130.57, 129.05, 128.03, 127.87, 127.63, 124.82, 120.54, 119.12, 109.81, 109.08, 108.90, 108.06, 107.86, 26.47, 24.53, 24.22, 24.01, 21.62, 13.92. ^{31}P NMR ($CDCl_3$, 160 MHz): δ 4.71 ($^1J_{Pt-P} = 3100$ Hz). Elem anal. calcd (%) for $C_{118}H_{157}N_4P_4Pt_2Zn$: C, 64.10; H, 7.16; N, 2.53. Found: C, 63.84; H, 6.88; N, 2.34.

5,15-Bis(*trans*-bis(1,4-ethynylbenzene)bis(tri-*n*-butylphosphine)-platinum(II))-10,20-bis(*n*-pentyl)zinc(II)porphyrin (M2). Treatment of **L2** (108 mg, 0.152 mmol) with 2 equiv of *trans*-phenylethynylchlorobis(tri*n*-butylphosphine)-platinum(II) (224 mg, 0.304 mmol) for 12 h at 298 K, in the presence of CuI (3 mg), in $^iPr_2NH-CH_2Cl_2$ (50 mL, 1:1, v/v) gave the title complex as a red solid in 38.4% yield (122 mg) after purification through column chromatography using silica and *n*-hexane/CH_2Cl_2 (40:60, v/v) as a solvent. ^{1}H NMR ($CDCl_3$, 400 MHz): δ 0.98−1.07 (m, 36 H), 1.53−1.65 (m, 28 H), 1.73−1.86 (m, 28 H), 2.28−2.36 (m, 24 H), 2.55−2.57 (m, 4 H), 5.00−5.05 (m, 4 H), 7.26−7.34 (m, 10 H), 7.68 (d, 4H, $J = 10.3$ Hz), 8.05 (d, 4H, $J = 10.7$ Hz), 9.02 (d, 4H, $J = 6.4$ Hz), 9.54 (d, 4H, $J = 6.1$ Hz). ^{13}C NMR ($CDCl_3$, 100 MHz): δ 150.12, 149.27, 139.84, 134.19, 132.09, 130.82, 128.89, 128.49, 127.86, 124.82, 120.48, 119.96, 109.47, 109.11, 108.90, 108.06, 38.76, 35.73, 32.87, 26.47, 24.52, 24.00, 22.84, 14.18, 13.95. ^{31}P NMR ($CDCl_3$, 160 MHz): δ 4.56 ($^1J_{Pt-P} = 3102$ Hz). Elem anal. calcd (%) for $C_{110}H_{157}N_4P_4Pt_2Zn$: C, 62.47; H, 7.48; N, 2.65. Found: C, 62.66; H, 7.70; N, 2.81.

Instrumentation. Infrared spectra were recorded as powder or THF solutions using a Perkin−Elmer Paragon 1000 PC or Nicolet Magna 550 Series II FTIR spectrometer, using CaF_2 cells with a 0.5 mm path length. NMR spectra were measured in appropriate deuterated solvents on a JEOL EX270 or a Varian Inova 400 MHz FT-NMR spectrometer, with ^{1}H NMR chemical shifts quoted relative to $SiMe_4$ and ^{31}P chemical shifts relative to an 85% H_3PO_4 external standard. Fast-atom bombardment (FAB) mass spectra were recorded on a Finnigan MAT SSQ710 mass spectrometer in *m*-nitrobenzyl alcohol matrices. The molecular weights of the polymers were determined by gel permeation chromatography (GPC; HP 1050 series HPLC with visible wavelength and fluorescent detectors) using polystyrene standards and THF as an eluent, and the thermal analyses were performed with a Perkin-Elmer TGA6 thermal analyzer. The UV/vis spectra were recorded on a Hewlett-Packard diode array model 8452 A at Sherbrooke. The emission and excitation spectra were obtained using a double monochromator Fluorolog 2 instrument from Spex. Phosphorescence time-resolved measurements were performed on a PTI LS-100 using a 1 ms tungsten flash lamp. Fluorescence and phosphorescence lifetimes were measured on a Timemaster Model TM-3/2003 apparatus from PTI. The source was a nitrogen laser with a high-resolution dye laser (fwhm $\approx$ 1.5 ns), and the fluorescence lifetimes were obtained from high-quality decays and deconvolution or distribution lifetime analysis. The uncertainties were about $\pm$40 ps on the basis of multiple measurements. The flash photolysis spectra and the transient lifetimes were measured with a Luzchem spectrometer using the 355 nm line of a YAG laser from Continuum (Serulite) and the 355 nm line from an OPO module pump of the same laser (fwhm = 13 ns).

Quantum Yield Measurements. For room-temperature measurements, all samples were prepared under an inert atmosphere (in a glovebox, $P_{O2} < 20$ ppm) by dissolution of the different compounds in 2MeTHF using 1 mL quartz cells with a septum (298 K) or quartz NMR tubes in liquid nitrogen for 77 K measurements. Three different measurements (i.e., different solutions) were performed for each set of photophysical data (quantum yields, Φ_F). The sample concentrations were chosen to correspond to an absorbance of 0.05 at the excitation wavelength. Each absorbance value was measured five times for better accuracy in the measurements of emission quantum yield (Φ_F). The Φ_F was tretraphenylporphyrin, H_2TPP ($\Phi_F = 0.11$ in 2MeTHF at 77 K),[17] which was checked against (Pd)TPP ($\Phi_F = 0.17$ in methylcyclohexane at 77 K).[18,19]

Crystallographic Data. The crystals were grown by slow vapor diffusion of hexanes in a CH_2Cl_2 solution. One single crystal of $0.50 \times 0.50 \times 0.60$ mm^3 was mounted using a glass fiber on the goniometer. Data were collected on an Enraf-Nonius CAD-4 automatic diffractometer using omega scans at 198(2) K. The DIFRAC[20] program was used for centering, indexing, and data collection. One standard reflection was measured every 100 reflections; no intensity decay was observed during data collection. The data were corrected for absorption by empirical methods based on ψ scans and reduced with the NRCVAX[21] programs. They were solved using SHELXS-97[22] and refined by full-matrix least-squares on F^2 with SHELXL-97.[23] The non-hydrogen atoms were refined anisotropically. The hydrogen atoms were placed at idealized calculated geometric position and refined isotropically using a riding model. The CH_2Cl_2 solvent molecule was disordered.

Results and Discussion

Synthesis and Characterization. *Meso*-substituted dipyrromethanes are synthesized from the reaction of a desired aldehyde in the presence of an excess of pyrrol (neat solvent) and a mild Lewis acid (e.g., $MgBr_2$) at room temperature.[24] The two functional groups, mesityl and *n*-pentyl, are used to test the solubility propensity of the target polymers. The condensation of 4-((trimethylsilyl)-ethynyl)benzaldehyde and 5-mesityldipyrromethane is initiated with $BF_3 \cdot O(Et)_2$ and subsequently quenched with DDQ (after 1 h). The free base porphyrins are then metalled with zinc(II) from zinc acetate (in a CH_2Cl_2/MeOH mixture refluxing 2 h) to form the trimethysilane-containing ethynyl derivatives **T1** and **T2**. The diethynyl zinc porphyrins **L1** and **L2** are then prepared by proton-desilylation using K_2CO_3 in MeOH as the base (Scheme 1).

Scheme 2 presents the synthesis scheme for the Pt(II)-containing polymers **P1** and **P2** and their model corresponding

(17) Strachan, J. P.; Gentemann, S.; Seth, J.; Kalsbeck, W. A.; Lindsey, J. S.; Holten, D.; Bocian, D. F. *J. Am. Chem. Soc.* **1997**, *119*, 11191.
(18) Harriman, A. *J. Chem. Soc. Faraday Trans. 2* **1981**, *77*, 1281.
(19) Murov, S. L.; Carmichael, I.; Hug, G. L. *Handbook of Photochemistry*, 2nd ed.; Marcel Dekker: New York, 1993.
(20) Flack, H. D.; Blanc, E.; Schwarzenbach, D. *J. Appl. Crystallogr.* **1992**, *25*, 455.
(21) Gabe, E. J.; Le Page, Y.; Charland, J.-P.; Lee, F. L.; White, P. S. *J. Appl. Crystallogr.* **1989**, *22*, 384.
(22) Sheldrick, G. M. *SHELXS-97*, release 97-2; Sheldrick, G. M., Ed.; University of Göttingen: Göttingen, Germany, 1997.
(23) Sheldrick, G. M. *SHELXL-97*, release 97-2; Sheldrick, G. M., Ed.; University of Göttingen: Göttingen, Germany, 1997.
(24) Laha, J. K.; Dhanalekshmi, S.; Taniguchi, M.; Ambroise, A.; Lindsey, J. S. *Org. Proc. Res. Dev.* **2003**, *7*, 799.

Scheme 1

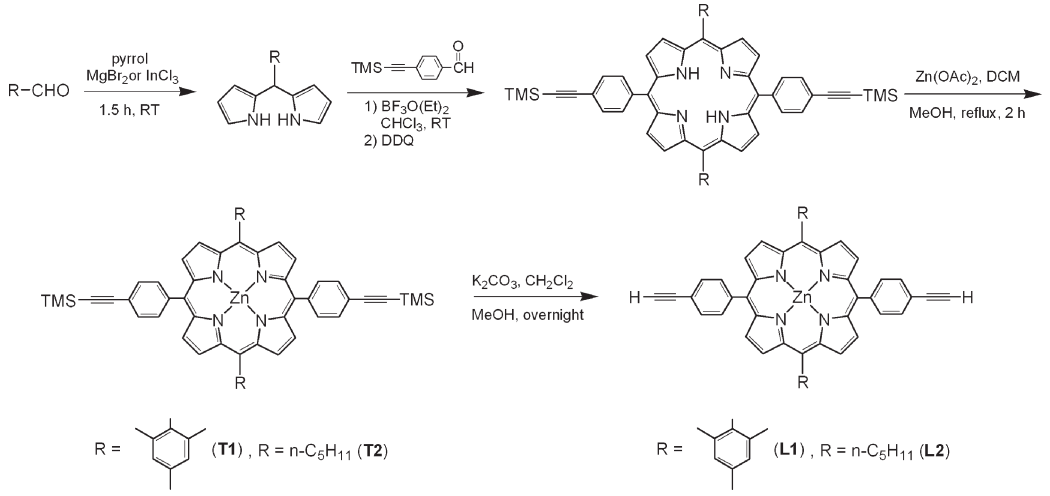

Scheme 2

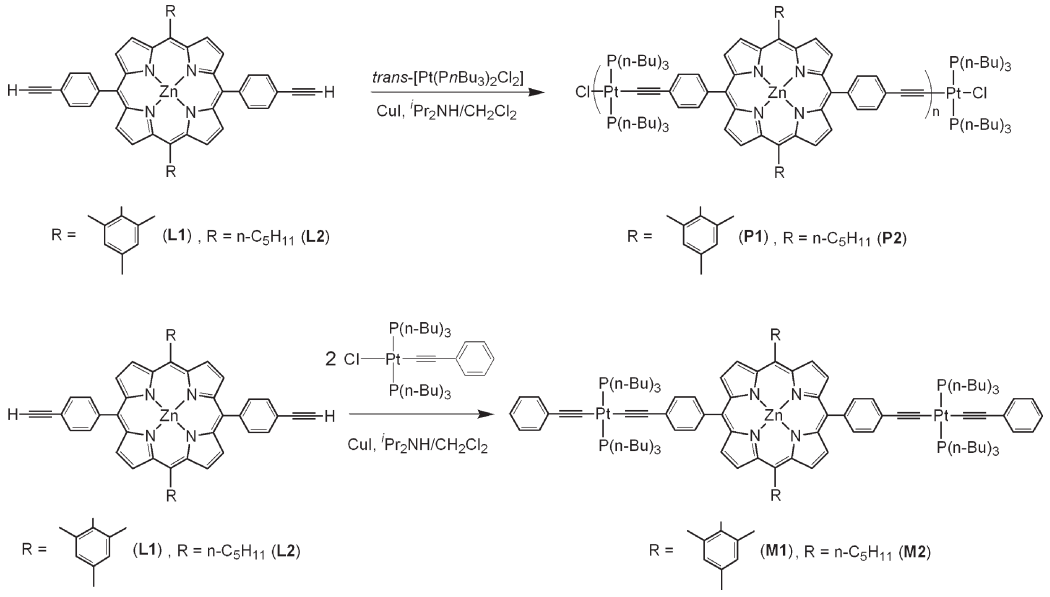

dinuclear complexes **M1** and **M2**. These species are prepared from the reaction of the ligands **L1** and **L2** with the Pt(II)-containing mono- and difunctional derivatives *trans*-Pt(P(*n*-Bu)$_3$)$_2$(C≡CC$_6$H$_5$)Cl and *trans*-Pt(P(*n*-Bu)$_3$)$_2$Cl$_2$ in the presence of the ethynyl-activating reactant CuI and a base (*i*-Pr$_2$NH). The desired Pt(II) diyne-containing model compounds are readily isolated using a silica column, whereas the purification of **P1** and **P2** is achieved by filtering the crude material through a short column using pure CH_2Cl_2 as the solvent. The polydispersity can be improved by precipitating the polymer-containing CH_2Cl_2 solution in MeOH. All of the new metal complexes and polymers are air-stable and generally exhibit good solubility in chlorocarbons such as CH_2Cl_2 and $CHCl_3$.

The solution IR spectra of these new metal complexes display a single sharp ν(C≡C) absorption peak (not two) in the range of 2100−2104 cm^{-1}, consistent with a trans configuration (i.e., D_{2h} symmetry) of the ethynylene ligands around the metal center. The absence of the C≡CH stretching mode of each compound at around 3300 cm^{-1} corroborates the successful formation of a M−C≡C bond. The NMR spectral data support the conclusion that these compounds have well-defined and symmetrical structures. The ^{31}P NMR spectra of the Pt(II)-containing complexes exhibit a single resonance with a pair of Pt satellites. Moreover, two distinct ^{13}C NMR signals for the individual sp carbons are observed, and they are shifted downfield with respect to the free ligands. The aromatic region in the ^{13}C NMR spectra reveals a high degree of structural regularity in the polymers. The observation of intense molecular ion peaks in the positive-ion FAB mass spectra confirms the formulas for **M1** and **M2**.

In order to prepare the investigated oligomers/polymers, the reaction time was kept constant at 12 h and the temperature was varied during the various runs between 20 and 110 °C. For the characterization of the resulting materials, GPC analysis was used to estimate the molecular weight of each polymer (see data in the Experimental Section). However, the data should be viewed with

Table 1. GPC Characterizations of **P1** and **P2**

polymer code	M_n	M_w	*n* (approximate length/nm)[a]	PD (M_w/M_n)
P1(*n* = 4)	5410	6270	4 (~10.0)	1.16
P1(*n* = 9)	13260	24530	9 (~22.5)	1.85
P2(*n* = 3)	3590	4940	3 (~7.5)	1.39
P2(*n* = 6)	7460	11500	6 (~15.0)	1.54
P2(*n* = 9)	11100	22140	9 (~22.5)	1.85

[a] Approximated average length of the oligomer (in nm) extracted from the X-ray dimension of a repetitive unit (see below for **M1**) multiplied by the average number of units. In this approximation, the end group is neglected since its exact nature is not known.

caution in view of the difficulties associated with utilizing GPC for rigid-rod polymers, which have appreciable differences in the hydrodynamic behavior from those for flexible polystyrene polymers (used as comparative standards). Hence, we would anticipate certain systematic discrepancies in the GPC measurements. However, the lack of discernible ^{1}H resonance and IR absorption attributed to the C≡C−H end groups in the NMR and IR spectra suggests the presence of a good degree of oligomerization for most of these materials, but for the shorter oligomers, the presence of *trans*-Pt(P(*n*-Bu)$_3$)$_2$Cl as end groups should be strongly suspected. Nonetheless, the number of units, *n*, varies from 3 to 9 (Table 1), and we did find a particular trend relating the synthesis conditions and the resulting average molecular dimension. For **P2**, for example, the temperatures were 20, 110, and 80 for $n = 3$, 6, and 9, respectively. Attempts were made to increase the polymer dimensions but all stubbornly failed, most likely due to the nature of the solubilizing side groups employed. So, these oligomeric/polymeric materials were investigated as such. The photoelectron diffraction (PD) is also found to be somewhat large (from 1.16 to 1.85) but is common for the type of reaction employed.

The thermal properties of two representative materials were investigated. Indeed, **P1(*n* = 9)** and **P2(*n* = 3)** were examined by thermal gravimetric analysis (TGA) under nitrogen (Figure 1). The TGA trace for **P1(*n* = 9)** exhibits a first weight loss at about 300 °C, indicative of its excellent thermal stability. The trace at a higher temperature is ill-defined, consistent with the polymeric nature of the solid. The TGA trace for **P2(*n* = 3)** exhibits a first weight loss around 280 °C, also showing a good thermal stability, but this trace differs from that recorded for **P1-(*n* = 9)**, where plateaus are noted with a fast weight loss at about 410 °C. The rapid weight loss represents 12−20% of the total mass of the M_n of **P2(*n* = 3)**. This may correspond to a loss of an end group Pt(P(*n*-Bu)$_2$)$_3$Cl (12%). The Cl represents only 0.7%. Moreover, polymers **P1-(*n* = 9)** and **P2(*n* = 3)** exhibit a glass transition at ~116 and 176 °C, respectively (DSC).

During the course of this investigation, one model compound, **M1**, crystallized to form crystals suitable for X-ray analysis (Figure 2). The geometry of the Pt(II)-containing organometallic fragment is the expected square planar, and the ligand environment exhibits a trans geometry, as spectroscopically demonstrated, consistent with the unique ν(C≡C) IR absorption. The bond distances are found to be normal (2.287 and 2.286 Å for Pt−P, 1.995 and 2.009 Å for Pt−C, and 2.039 Å for Zn−N, for example). The angle between the xylyl and

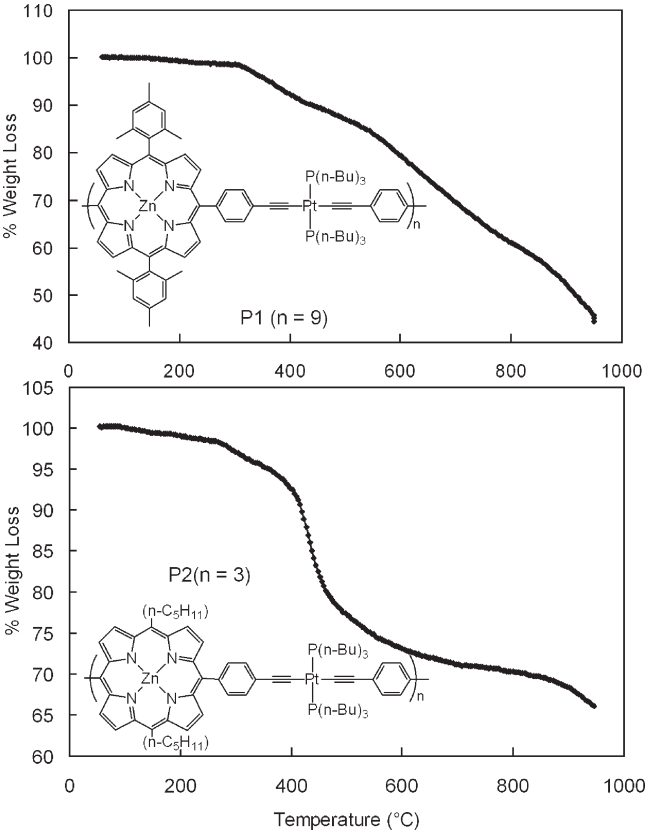

Figure 1. TGA traces for **P1(*n* = 9)** and **P2(*n* = 3)** (heating rate: 20 °C min^{-1}). The end groups are not shown on the structures for convenience.

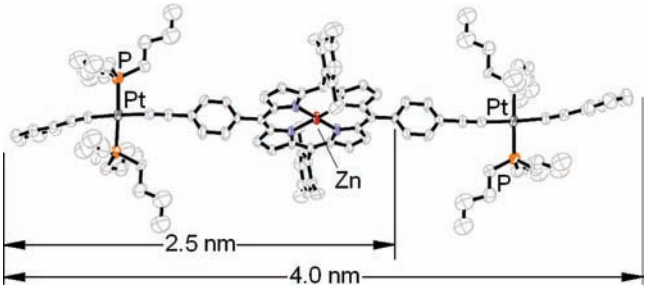

Figure 2. ORTEP representation of **M1**. The thermal ellipsoids are presented at 50% probability. The H atoms and solvent crystallization molecule are omitted for clarity.

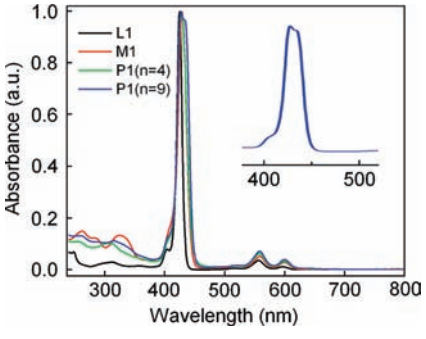

Figure 3. Normalized UV−vis spectra of **L1**, **M1**, **P1(*n* = 4)**, and **P1(*n* = 9)** in 2MeTHF (298 K). Inset: expansion of the spectrum for **P1(*n* = 9)** stressing the splitting of the Soret band.

Table 2. UV−Vis Absorption Data in 2MeTHF at 298 K

	λ_{max} [nm] ($\varepsilon \times 10^{-3}$ M^{-1} cm^{-1})[a]				
compds.	Soret region		Q bands		
M1	263, 284, 326	429 (454.8)	519 (4.6)	558 (22.4)	599 (11.9)
M2	262, 286, 327	431 (93.0)	522 (2.4)	561 (4.6)	604 (3.9)
P1(*n* = 4)	256, 312	427 (396.7), ∼430(sh)	519 (4.7)	558 (21.7)	600 (10.4)
P1(*n* = 9)	261, 315	427 (204.1), 435(sh)	518 (2.1)	558 (10.2)	599 (5.2)
P2(*n* = 3)	264, 289, 317, 338	434 (226.6), 424(sh)	522 (2.7)	561 (12.0)	606 (9.7)
P2(*n* = 6)	284, 321	434 (142.2), 425(sh)	520 (3.54)	561 (10.5)	605 (8.7)
P2(*n* = 9)	264, 282, 327	433 (235.5), 426 (sh)	525 (2.7)	561 (14.4)	604 (12.3)
L1	249, 313	404 (69.3), 425 (923)	517 (5.7)	556 (33.1)	597 (10.1)
L2	248, 314	405 (30.9), 426 (321)	521 (2.1)	559 (12.2)	604 (6.7)

[a] The absorptivities for the oligomers were calculated using concentrations based on the mass of a repetitive unit.

porphyrin planes is 81.51°, whereas that for the phenyl and porphyrin is 86.7°, strongly suggesting a weak conjugation between the two chromophores. The angle made by the average plane of the porphyrin and the P−P axis is 64.1°. The angle made by the average porphyrin plane and the Pt−Pt axis is 6.1°, suggesting that these molecular objects can be treated as relatively rigid sticks.

This structure also provides the opportunity to measure the average length of the target oligomers. The total distance of **M1** (outmost *para*-H to *para*-H) is ∼ 40 Å (4.0 nm). The length of a repetitive unit ([$(C_6H_5C{\equiv}C)$Pt-$(P(n\text{-}Bu)_3)_2(C{\equiv}C\text{-}p\text{-}C_6H_4)$**Zn(P)**]; **Zn(P)** = zincporphyrin) is ∼ 25 Å (2.5 nm), as measured from the outmost *para*-H and the first carbon atom of the phenyl group, as illustrated in Figure 2. Using this measurement, the average oligomer lengths are estimated using *n*, the number of units, extracted from M_n (GPC; Table 1). These vary from 7.5 to 22.5 nm.

Spectroscopic and Photophysical Properties. Absorption spectra. The ligands **L1** and **L2**, model compounds **M1** and **M2**, and oligomers **P1** and **P2** exhibit similar absorption spectra (Figure 3 for **L1**, **M1**, **P1(*n* = 4)**, and **P1(*n* = 9)** as typical examples, see also Table 2).

The spectra are characterized by three regions. The $\pi\pi^*$-type Q (500−600) and Soret (400−450 nm) bands are characteristic of the porphyrin macrocycles. The third region, 250−400 nm, exhibits lower-intensity bands belonging to both the porphyrin unit and the [$(p\text{-}C_6H_4$-$C{\equiv}C)Pt(P(n\text{-}Bu)_3)_2(C{\equiv}C\text{-}p\text{-}C_6H_4)$] moiety. The assignment for the lowest-energy UV band for this latter Pt-containing unit is a mixture of ligand-to-metal charge transfer and a metal-to-ligand charge transfer where M is the Pt atom and L represents the phenylethynyls, as recently demonstrated for analogous conjugated organometallic polymers (Chart 2, see ref 25 for examples and the references therein).[25]

The examination of the peak maxima of Q bands indicates that there is essentially no red-shift as the number of repetitive units increases. This observation indicates that these polymers are more or less not conjugated along the chain. All in all, each chromophore appears π-separated from the others, which is entirely consistent with the quasi perfect right angle made by the average planes of the porphyrin ring and the aryl groups

Chart 2

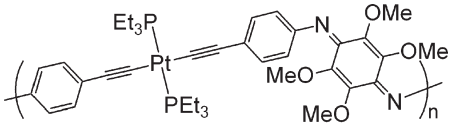

lumophore electron acceptor

around the central macrocyle in the solid state. On the other hand, the Soret bands for **P1** and **P2** exhibit two components that become clearer as the number of units increases (see inset). This is due to an exciton coupling, well-known in linear oligomers and polymers of porphyrins.[26]

Luminescence spectra. The photophysical data for all compounds are summarized in Tables 3 and 4, and the emission spectra are shown in Figure 2. The two chromophores, **Zn(P)** (with **P** = porphyrin chromophore), known to be strongly fluorescent,[27,28] and *trans*-$(C_6H_5C{\equiv}C)$Pt-$(P(n\text{-}Bu)_3)_2(C{\equiv}C\text{-}p\text{-}C_6H_5)$, which is strongly phosphorescent, namely, at 77 K, were monitored at 298 and 77 K.[25]

For all cases at 298 K in 2MeTHF, the emission spectra are dominated by the intense fluorescence arising from the ZnP unit ($\lambda_{0,0} \approx 610$ nm for **M1** and **P1**, $\lambda_{0,0} \approx 616$ nm for **M2** and **P2**). Weaker fluorescence and phosphorescence arising from the *trans*-$(p\text{-}C_6H_4C{\equiv}C)Pt(P(n\text{-}Bu)_3)_2(C{\equiv}C\text{-}p\text{-}C_6H_4)$ spacer are depicted in the 400 and 500 nm regions, respectively. Whereas the position of the phosphorescence $\lambda_{0,0}$ peak ($\approx$ 445 nm) of the *trans*-$(p\text{-}C_6H_4C{\equiv}C)Pt(P(n\text{-}Bu)_3)_2(C{\equiv}C\text{-}p\text{-}C_6H_4)$ unit remains relatively constant for all investigated compounds and polymers at 298 K (except for a slight red-shift with the molecular dimension), the band shape changes somewhat for the oligomer where some vibronic components exhibit an increase in intensity. Similarly, the $\lambda_{0,0}$ of the ZnP fluorescence undergoes a relatively modest red-shift going, for example, from 606 to 610, 610, and 611 nm for **L1**, **M1**, **P1(*n* = 4)**, and **P1(*n* = 9)**, respectively (the total shift is 5 nm or 135 cm^{-1}), indicating that the conjugation is moderate. This is again consistent with the X-ray structure of the model complex **M1** where a quasi-right angle is made by the average planes of the

(25) Gagnon, K.; Aly, S. M.; Wittmeyer, A. B.; Bellows, D.; Bérubé, J. F.; Caron, L.; Abd-El-Aziz, A. S.; Fortin, D.; Harvey, P. D. *Organometallics* **2008**, *27*, 2201.

(26) Harvey, P. D. *The Porphyrin Handbook*; Kadish, K. M., Smith, K. M., Guilard, R., Eds.; Academic Press: San Diego, 2003; Vol. *18*, pp 63−250.

(27) M. Gouterman, M. In *The Porphyrins*; Dolphin, D., Ed.; Academic Press: New York, 1978; Vol. *III*, p 1.

(28) Seybold, P. G.; Gouterman, M. *J. Mol. Spectrosc.* **1969**, *31*, 1.

Table 3. Fluorescence and Phosphorescence Data

	λ_{max} [nm][a]		Φ_e (±10%)[b]	
compd. or polymer	298 K	77 K	298 K	77 K
M1	[Pt]: fluo: 391; phos: 449 ZnP: fluo: 610, 660	[Pt] fluo: 385, 397; phos: 416, 446, 473, 496 ZnP fluo: 599, 656, 724; phos: 788	0.125	0.121
M2	[Pt]: fluo: 397; phos: 446, 511 ZnP: fluo: 616, 665	[Pt]: phos: 446, 467, 481, 493 ZnP: fluo: 610, 637, 667; phos: 815 w	0.047	0.081
P1(n = 4)	[Pt]: fluo: 392; phos: 438 ZnP: fluo: 610, 658	[Pt]: fluo: 393, 413; phos: 451, 472, 500, 530 ZnP: fluo: 604, 662, 714; phos: 797 w	0.071	0.062
P1(n = 9)	[Pt]: fluo: 390; phosp: 452 ZnP: fluo: 611, 659	[Pt]: fluo: 398, 413; phos: 452, 471, 498, 530 ZnP: fluo: 606, 662, 723; phos: 803 w	0.080	0.120
P2(n = 3)	[Pt]: fluo: 385; phos: 441, 510 ZnP: fluo: 616, 664	[Pt]: phos: 447, 471, 502, 523, 533 ZnP: fluo: 612, 630, 666; phos: 815 w	0.081	0.163
P2(n = 6)	[Pt]: fluo: 396; phos: 446 ZnP: fluo: 616, 664	[Pt]: fluo: 397, 418; phos: 446, 470, 490 ZnP: fluo: 614, 669, 731 w; phos: 822 w	0.086	0.17
P2(n = 9)	[Pt]: fluo: 396; phos: 446 ZnP: fluo: 616, 662	[Pt]: fluo: 393, 418; phos: 450, 472, 495, 523 ZnP: fluo: 615, 638, 667, 703; phos: 823 w	0.051	0.065
L1	ZnP: fluo: 606, 656, 720	ZnP: fluo: 598, 654, 715; phos: 792 w	0.074	0.060
L2	ZnP: fluo: 612, 664, 726	ZnP: fluo: 605, 663; phos: 795 w	0.098	0.11

[a] Chromophore ZnP = zinc(II)porphyrin, chromophore [Pt] = *trans*-($C_6H_4C{\equiv}C$)Pt($P(n\text{-}Bu)_3$)$_2$($C{\equiv}C\text{-}p\text{-}C_6H_4$). [b] Total Φ_e of the ZnP chromophore (i.e., fluorescence), λ_{exc} = 560 nm.

Table 4. Fluorescence and Phosphorescence Lifetimes and Rate Constants for T_1 ET[a]

	lifetime			
compd. in 2MeTHF	τ_F(ns) 298 K[b]	τ_P(μs) 77 K	τ_F(ns) 77 K	k_{ET} λ_{exc} = 345 nm (10^4 s^{-1}) 77 K
standard		35.0 ± 1.3 [Pt][c]		
L1	1.18 ± 0.06 ZnP	29800 ± 4000 ZnP	3.10 ± 0.03 ZnP	
L2	1.11 ± 0.09 ZnP	21100 ± 1890 ZnP	3.34 ± 0.02 ZnP	
M1	1.28 ± 0.05 ZnP	11800 ± 830 ZnP	2.56 ± 0.08 ZnP	
		12.6 ± 0.8 [Pt]		5.1 ± 0.6
M2	0.60 ± 0.10 ZnP	13600 ± 1380 ZnP	2.81 ± 0.04 ZnP	
		18.8 ± 1.4 [Pt]		2.4 ± 0.6
P1(n = 4)	1.00 ± 0.18 ZnP	14000 ± 500 ZnP	2.29 ± 0.05 ZnP	
		13.2 ± 1.7 [Pt]		4.7 ± 1.0
P1(n = 9)	0.93 ± 0.29 ZnP	8400 ± 13 ZnP	2.38 ± 0.02 ZnP	
		10.5 ± 0.8 [Pt]		6.7 ± 1.0
P2(n = 3)	0.66 ± 0.02 ZnP	11900 ± 510 ZnP	2.49 ± 0.06 ZnP	
		12.3 ± 2.5 [Pt]		5.3 ± 1.5
P2(n = 6)	0.55 ± 0.01 ZnP	10900 ± 500 ZnP	2.08 ± 0.03 ZnP	
		2.9 ± 0.7 [Pt]		32 ± 7
P2(n = 9)	0.51 ± 0.07 ZnP	8340 ± 300 ZnP	2.51 ± 0.04 ZnP	
		0.73 ± 0.07 [Pt]		130 ± 20

[a] Chromophore ZnP = zinc(II)porphyrin, chromophore [Pt] = *trans*-($C_6H_4C{\equiv}C$)Pt-($P(n\text{-}Bu)_3$)$_2$($C{\equiv}C\text{-}p\text{-}C_6H_4$). Their corresponding emission lifetimes were measured using the same excitation wavelengths as indicated in Figure 4. [b] The τ_P data of the [Pt] chromophore at 298 K could not be accurately measured because of the weakness of its emission intensity. [c] Value extracted from ref 25.

aryls and the porphyrin macrocycle. No phosphorescence arising from the ZnP chromophore is seen at 298 K.

At 77 K, all of these previous observations are also noted, but at this temperature, a very weak phosphorescence of the ZnP macrocycle now appears at ~800 nm (Figure 4). Moreover, the $\lambda_{0,0}$ of the ZnP fluorescence also undergoes a modest red-shift but somewhat relatively larger than that at 298 K, going for example from 598 to 599, 604, and 606 nm for **L1**, **M1**, **P1(n = 4)**, and **P1(n = 9)**, respectively (total shift is 8 nm or 220 cm^{-1}), indicating that the conjugation is slightly accentuated at 77 K. The change in band shape of the *trans*-(p-$C_6H_4C{\equiv}C$)Pt-($P(n\text{-}Bu)_3$)$_2$($C{\equiv}C\text{-}p\text{-}C_6H_4$) phosphorescence band is also notable (Figure 4). This observation, along with the (modest) red shift of the 0−0 peak with the molecular dimension, also corroborates the presence of some extended conjugation at this temperature. To explain this result, the presence of a change in dihedral angle between the aryl and porphyrin macrocycle average plane must take place.

Emission Lifetimes and Triplet State Energy Transfer. Photoinduced energy transfer processes in conjugated polymers containing the fragment *trans*-(p-$C_6H_4C{\equiv}C$)Pt-($P(n\text{-}Bu)_3$)$_2$($C{\equiv}C\text{-}p\text{-}C_6H_4$) and related derivatives,[25,29] and dyads containing the ZnP chromophore,[30] have been reported before and can be used as a basis for interpretation. The assignment of the energy donor and acceptor centers is appropriately made on the basis of the 0−0 peaks (Figure 4 and Table 4) of the fluorescence and phosphorescence bands. The upper energy donor and lower acceptor are the (*trans*-(p-$C_6H_4C{\equiv}C$)Pt($P(n\text{-}Bu)_3$)$_2$($C{\equiv}C\text{-}p\text{-}C_6H_4$)) and ZnP chromophores, respectively (Figure 5).

(29) Fortin, D.; Clement, S.; Gagnon, K.; Berubé, J.-F.; Stewart, M. P.; Geiger, W. E.; Harvey, P. D. *Inorg. Chem.* **2008**, *87*, 103.
(30) Faure, S.; Stern, C.; Espinosa, E.; Douville, J.; Guilard, R.; Harvey, P. D. *Chem. Eur. J.* **2005**, *11*, 3469.

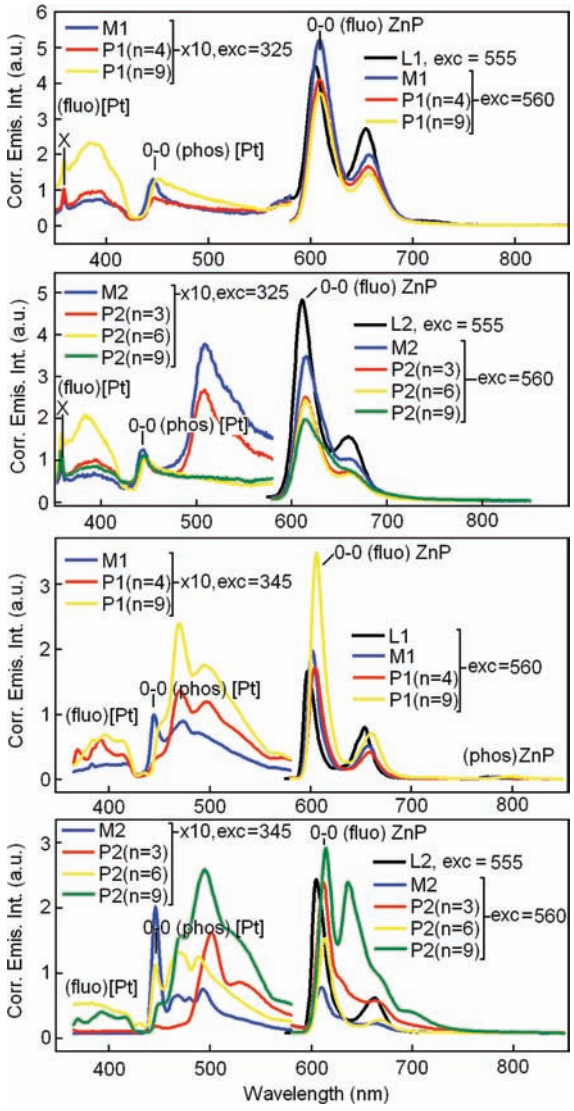

Figure 4. Top: Corrected emission spectra of **L1**, **M1**, **P1(*n*=4)**, and **P1 (*n* = 9)** at 298 K in 2MeTHF. Second: Corrected emission spectra of **L2**, **M2**, **P2(*n* = 3)**, **P2(*n* = 6)**, and **P2(*n* = 9)** at 298 K in 2MeTHF. Third: Corrected emission spectra of **L1**, **M1**, **P1(*n* = 4)**, and **P1(*n* = 9)** at 77 K in 2MeTHF. Bottom: Corrected emission spectra of **L2**, **M2**, **P2(*n* = 3)**, **P2 (*n* = 6)**, and **P2(*n* = 9)** at 77 K in 2MeTHF. The λ_{exc} values are indicated in the spectra. X = artifact; [Pt] = *trans*-(*p*-$C_6H_4C{\equiv}C$)Pt($P(n\text{-}Bu)_3$)$_2$-($C{\equiv}C$-*p*-C_6H_4); ZnP = zinc(II)porphyrin; (fluo) = fluorescence; (phos) = phosphorescence.

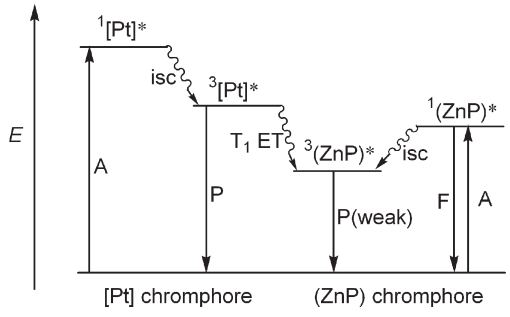

Figure 5. Energy diagram for the [Pt($P(n\text{-}Bu)_3$)$_2$C≡C(*p*-C_6H_4)**Zn(P)**(*p*-C_6H_4)C≡C]$_n$ polymers and the [($C_6H_5C{\equiv}C$)Pt($P(n\text{-}Bu)_3$)$_2$(C≡C-*p*-C_6H_4)-**Zn(P)**(*p*-C_6H_4)C≡CPt-($P(n\text{-}Bu)_3$)$_2$(C≡CC_6H_5)] model compounds ([Pt] = (*p*-C_6H_4)C≡CPt($P(n\text{-}Bu)_3$)$_2$C≡C(*p*-C_6H_4)). The relevant radiative (A=absorbance, F=fluorescence, P=phosphorescence) and nonradiative (isc = intersystem crossing, T_1 ET=triplet energy transfer) are indicated.

Chart 3. Standard (*trans*-(PhC≡C)Pt($P(n\text{-}Bu)_3$)$_2$(C≡CPh))[25]

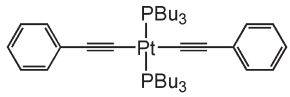

Standard (*trans*-(PhC≡C)Pt($P(n\text{-}Bu)_3$)$_2$(C≡CPh))[25]

Taking into account the uncertainties, the τ_F data of the zinc(II)porphyrin chromphore (depicted as ZnP in Table 3) for **L1** → **M1** → **P1(*n* = 4)** → **P1(*n* = 9)** and **L2** → **M2** → **P2(*n* = 3)** → **P2(*n* = 6)** → **P2(*n* = 9)** at both temperatures reveal a slight decrease in τ_F. The most notable change in τ_F data concerns the passages **L1** → **M1** and **L2** → **M2**, where a decrease is noted at 77 K. This decrease is assigned to a heavy atom effect (due to the incorporation of the Pt atoms in the chain) and the lengthening of the oligomeric chains, adding vibrational modes for nonradiative excited state deactivation. The τ_P data of the zinc(II)porphyrin chromphore show the same tendency (i.e., a decrease in τ_P according to **L1** → **M1** → **P1(*n* = 4)** → **P1(*n* = 9)** and **L2** → **M2** → **P2(*n* = 3)** → **P2-(*n* = 6)** → **P2(*n* = 9)**), which is also due to a heavy effect, which is also particularly notable for the passages **L1** → M1 and **L2** → **M2**, and the lengthening of the oligomeric chains. These variations in τ_F and τ_P data of the ZnP chromphore occur by a factor of about 2, at the most, considering the uncertainties.

The τ_P data for the *trans*-($C_6H_4C{\equiv}C$)Pt($P(n\text{-}Bu)_3$)$_2$-($C{\equiv}C$-*p*-C_6H_4) chromophore (i.e., [Pt]) along the same series also exhibit a more important decrease and heavy atom effect, and the oligomer chain cannot explain this larger change. In comparison with the nonfunctionalized spacer *trans*-(PhC≡C)Pt($P(n\text{-}Bu)_3$)$_2$(C≡CPh) (see standard in Chart 3), the τ_P values change from 35 μs[25] down to 10.5 (>3 times) and 0.73 μs (>45 times) for **P1(*n* = 9)** and **P2(*n* = 9)**, respectively, hence representing larger decreases. These supplementary nonradiative processes promoting excited deactivation of the spacer emission are T_1 ET. The photoinduced electron transfer is unlikely at 77 K in glassy matrices (because of the very large reorganization energy) and is rather rare in the triplet excited states.

Evidence for T_1 ET is provided by means of measurements of the transient absorption spectra on the microsecond time scale (see **L1** and **M1** for examples; Figure 6). In the $T_1{-}T_n$ absorption spectrum of **L1**, for which no electron transfer is possible, a broad and dissymmetric band is noted at about 450 nm. For **M1**, the same band is observed plus a feature at 800 nm. The latter feature is due to the $T_1{-}T_n$ absorption band of the *trans*-(*p*-$C_6H_4C{\equiv}C$)Pt($P(n\text{-}Bu)_3$)$_2$(C≡C-*p*-C_6H_4) unit, on the basis of the literature (see ref 25 and the references therein).

So the transient absorption spectra at 77 K are consistent with $T_1{-}T_n$ absorption signatures with no evidence for charge-separated state, as no other feature is observed. The rate of energy transfer (k_{ET}) is quantified by $k_{ET} = (1/\tau_e) - (1/\tau_e^\circ)$, where τ_e is the emission lifetime of the donor in a system where the donor is involved in an intramolecular energy transfer process and τ_e° is the emission lifetime of the donor in the absence of an energy transfer.[26] In this work, τ_e would be, for **M1**, **M2**, **P1**, and **P2**, excited at 345 nm (at 77 K) and τ_e° would be for

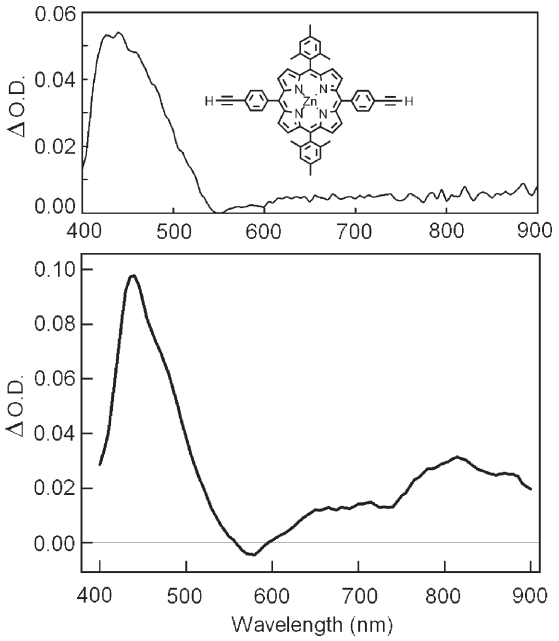

Figure 6. Transient absorption spectra of **L1** (top) and **M1** (bottom) in 2MeTHF at 77 K excited at 355 nm (delay = 1 μs). The transient absorption band at 800 nm is the T_1-T_n absorption of the *trans*-(*p*-C_6H_4-C≡C)Pt(P(*n*-Bu)$_3$)$_2$(C≡C-*p*-C_6H_4) spacer.

trans-(PhC≡C)Pt(P(*n*-Bu)$_3$)$_2$(C≡CPh) (i.e., 35 μs).[25] The extracted k_{ET} values (Table 3) reveal a modest and more pronounced decrease going from **M1** → **P1(*n* = 4)** → **P1-(*n* = 9)** and **M2** → **P2(*n* = 3)** → **P2(*n* = 6)** → **P2(*n* = 9)**, respectively. The latest series exhibits a change of 2 orders of magnitude for T_1 k_{ET}, but overall, these rates are respectively modest (10^4 s^{-1}) and relatively faster (10^6 s^{-1}) for these two series. Literature data for porphyrin-containing assemblies reveal that T_1 k_{ET} ranges typically between 10^3 and 10^9 s^{-1}.[26] As for the reason as to why one substituent (*n*-pentyl) leads to faster T_1 energy transfers (in comparison with the mesityl) as the chain length increases is unknown. However, one may speculate that the flexible chain of the *n*-pentyl side substitutes may induce a "loose bolt" effect,[31] rapidly draining the excited state energy by nonradiative pathways (interconversion from the triplet manifold) down to the ground state. If this is the case, one localized excited zinc(II)porphyrin being deactivated by remote *n*-pentyl groups is most unlikely. The only way to explain this effect is to have an exciton process allowing delocalization of the triplet state excitation,[32] hence having the excited chromophore more efficiently subjected to excited deactivation by the "loose bolt" effect. Evidence for exciton phenomena was previously provided and discussed by Schanze and his collaborators,[33] so it is not new. However, we find in these two series that the delocalization of this energy spreads over at least nine units, which is longer than that mentioned by Schanze (a few units) in the triplet excited states. It is also interesting to note that this jump (i.e., energy migration from one ZnP chromophore to another) operates over 18 Å (the $C_{meso}-$[spacer]$-C_{meso}$ separation; distance extracted from X-ray data for other spacers).[25]

Conclusion

A series of 1-D nanometer-sized oligomers built upon a metalloporphyrin and a rigid linear and conjugated organometallic spacer were prepared and characterized. Moderate variations of the photophysical data, notably the emission lifetimes of the metalloporphyrin chromophore (2 folds), are observed when in the presence of heavy atom effects (Pt) and when submitted to nonradiative pathways associated with the increase in chain length. However, when the excitation takes place directly in the absorption band of the *trans*-(*p*-C_6H_4C≡C)Pt(P(*n*-Bu)$_3$)$_2$(C≡C-*p*-C_6H_4) spacer, T_1 ET operates from the spacer (donor) to the zinc(II)porphyrin (acceptor) with rates, k_{ET}, ranging from 10^4 (slow) to 10^6 s^{-1} (intermediate rate). The k_{ET} measurements are interesting since a dependence on the oligomer length is noticed. This work represents a basic example of the antenna effect (multichromophoric structure with electronic interactions) responsible for harvesting the light and for the migration of the light energy across a membrane or a material.

It is also interesting to note that the (−chromophore−spacer−)$_n$ topology bears some resemblance to the light-harvesting devices in photosystems of some photosynthetic bacteria. For example, the purple photosynthetic bacteria exhibit an LH II device (light-harvesting device II) where a circular structure of a little bit more than 10 nm composed of 18 bacteriochlorophylls a (B850), nine bacteriochlorophylls a (B800), and nine glucoside rhodopins (carotenoids) form a circular grid with upper (18 bacteriochlorrophylls) and lower rings (alternating nine bacteriochlorophylls and nine carotenoids) connected by the nine perpendicularly placed carotenoids.[34] All of the components act as molecular antenna for harvesting light and channeling this energy toward the reaction center protein (inside LH I). Exciton processes between the B800 units, which are separated by ~20 Å (Mg···Mg), occur at an efficient time scale of 500 fs. Here, the metalloporphyrin and the *trans*-(*p*-C_6H_4C≡C)Pt(P(*n*-Bu)$_3$)$_2$(C≡C-*p*-C_6H_4) spacer, although placed in a 1-D arrangement, play the roles of bacteriochlorophylls and carotenoids, respectively, for the lower ring. The presence of excitonic processes was evidenced here, where the rate of energy migration gets faster when the number of unit increases.

Acknowledgment. This research was supported by the Natural Sciences and Engineering Research Council of Canada (NSERC), le Fonds Québécois de la Recherche sur la Nature et les Technologies (FQRNT), and the Centre d'Études des Matériaux Optiques et Photoniques de l'Université de Sherbrooke (CEMOPUS). L.L. acknowledges the National Natural Science Foundation of China (No.20671033) for the purchase of her airplane tickets.

Supporting Information Available: This material is available free of charge via the Internet at http://pubs.acs.org.

(31) Turro, N. J. *Modern Molecular Photochemistry*; Benjamin/Cummings: Menlo Park, CA, 1978.
(32) Fortin, D.; Turcotte, M.; Drouin, M.; Harvey, P. D. *J. Am. Chem. Soc*. **1997**, *119*, 531.
(33) (a) Glusac, K.; Köse, M. E.; Jiang, H.; Schanze, K. S. *J. Phys. Chem. B* **2007**, 111. (b) Müller, J. G.; Atas, E.; Tan, C.; Schanze, K. S.; Kleiman, V. D. *J. Am. Chem. Soc*. **2006**, *128*, 4007.
(34) Harvey, P. D.; Stern, C.; Gros, P. C.; Guilard, R. *J. Inorg. Biochem*. **2008**, *102*, 395.